

Binding energy of the impurity level in the $\text{Ga}_{1-x}\text{Al}_x\text{As-GaAs-Ga}_{1-y}\text{Al}_y\text{As}$ superlattice

Kazuyoshi Tanaka

*Department of Hydrocarbon Chemistry, Faculty of Engineering, Kyoto University, Sakyo-ku, Kyoto 606, Japan
and Division of Molecular Engineering, Graduate School of Engineering, Kyoto University, Kyoto 606, Japan*

Masataka Nagaoka

Department of Hydrocarbon Chemistry, Faculty of Engineering, Kyoto University, Sakyo-ku, Kyoto 606, Japan

Tokio Yamabe

*Department of Hydrocarbon Chemistry, Faculty of Engineering, Kyoto University, Sakyo-ku, Kyoto 606, Japan
and Division of Molecular Engineering, Graduate School of Engineering, Kyoto University, Kyoto 606, Japan*

(Received 19 July 1983)

The binding energy of the first impurity level in the $\text{Ga}_{1-x}\text{Al}_x\text{As-GaAs-Ga}_{1-y}\text{Al}_y\text{As}$ superlattice is investigated by considering a variational problem in a finite quantum well with a hydrogenic impurity potential. For the case of the finite well, we first deal with the dependency of the binding energy on the impurity position and on the barrier heights of the quantum well. Each barrier height is independently changed in the present study. It is pointed out that the binding energy is underestimated when one employs an infinite barrier height to represent the quantum well. The electron distribution in the superlattice depending on various impurity positions is also discussed.

I. INTRODUCTION

Recently much attention has been paid to the tailored constitution of thin layers of semiconductors or the superlattices first proposed by Esaki and Tsu.¹ In this substance, the bottom of the conduction band and the top of the valence band vary periodically in an oscillatory manner along a specific spatial direction, that is, perpendicular to each thin layer of the semiconductor. This is called the superlattice direction. The peculiar electronic structure manifested by the superlattices not only offers many interesting usages in the field of electronic devices, but accelerates the progress of scientific understanding.

From a theoretical point of view, Bastard first treated the hydrogenic impurity states in the quantum well representing the $\text{GaAs-Ga}_{1-x}\text{Al}_x\text{As}$ superlattice.² In his approach, however, the barrier height of the quantum well has been assumed to be infinite, that is, the tunneling effect across the interface of the layers has been completely neglected.

Mailhiot *et al.*³ and Greene and Bajaj⁴ have independently studied the energy levels of the hydrogenic impurity states in the $\text{GaAs-Ga}_{1-x}\text{Al}_x\text{As}$ superlattice system with a finite barrier height. Both of these calculations, however, have excluded the case of the impurity location outside the GaAs layer, that is, the case of the modulation doping, which is the most important way of doping in order to achieve a high electron mobility parallel to a superlattice layer.⁵

Hence, in this paper, we mainly study the dependence of the hydrogenic impurity state on the impurity site being outside the GaAs layer with respect to the binding energy and the density distribution of the injected electron into the GaAs layer. Moreover, we also investigate the effect of the different barrier height structure in the super-

lattice on these properties. Although this effect has never been discussed, it is expected to present crucial information on the preparation of practical devices based on the superlattice from an applicational point of view.

II. METHOD OF CALCULATION

We should like to consider a superlattice system consisting of the $\text{Ga}_{1-x}\text{Al}_x\text{As-GaAs-Ga}_{1-y}\text{Al}_y\text{As}$ structure as shown in the upper section of Fig. 1. In the present model the components (variables) x and y representing the content of Al can be varied independently, and the width of the GaAs layer is designated by L . The model potential in the lower section of Fig. 1 is employed to describe the

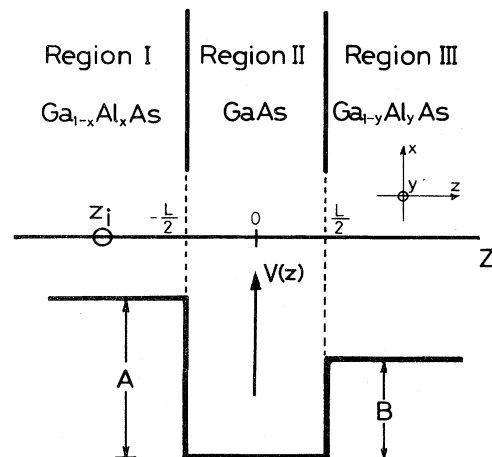


FIG. 1. Schematic representation of the model potential of the $\text{Ga}_{1-x}\text{Al}_x\text{As-GaAs-Ga}_{1-y}\text{Al}_y\text{As}$ superlattice.

quantum-well structure manifested by this superlattice. A hydrogenic impurity providing an electron that behaves as a carrier in the quantum well (region II) is located at an arbitrary point on the z axis in the present model. This feasibility is crucial to assess the case of the modulation doping, that is, when the impurity is buried in the region I or III. This case has been excluded in earlier studies.^{3,4}

Representing the site of the impurity by z_i , the Hamiltonian is written as follows in the framework of the effective-mass approximation:^{6,7}

$$H = -\frac{\hbar^2}{2m^*}\Delta + V(z) - \frac{e^2}{\epsilon[\rho^2 + (z - z_i)^2]^{1/2}}, \quad (1)$$

where

$$V(z) = \begin{cases} A = \hbar^2 a / 2m^*, & z < -L/2 \\ 0, & -L/2 < z < L/2 \\ B = \hbar^2 b / 2m^*, & z > L/2. \end{cases} \quad (2)$$

In Eq. (1) m^* is the effective mass of the carrier, ϵ is the dielectric constant of the material of interest, and $\rho [= (x^2 + y^2)^{1/2}]$ is the distance in the layer plane measured from the impurity site. Strictly speaking, the values of m^* and ϵ vary across the boundary between the two materials. However, since the carrier is to be confined in the GaAs layer (to a large extent due to the considerable barrier heights), it seems to be a good approximation to use the values of m^* and ϵ in GaAs in all regions of the superlattice.⁴ The relationship between A and x (B and y) is employed after Ref. 2. We assume, somewhat arbitrarily, that this holds up to $x=0.6$. It is in the present study that the effect of the different barrier heights is first considered. Thus the following expressions are employed throughout this study:

$$m^* = 0.067m_0, \quad (3a)$$

$$\epsilon = 12.0\epsilon_0, \quad (3b)$$

$$A = 1.06x, \quad (3c)$$

$$B = 1.06y, \quad (3d)$$

where m_0 and ϵ_0 are the values of the mass of a free electron and the dielectric constant in the vacuum, respectively.

The binding energy $E(L, z_i, \lambda)$ felt by an electron injected from the impurity is defined by the difference of the eigenenergy E_0 of the Hamiltonian in Eq. (1) without the third term in the right-hand side and that of (1), $\epsilon(L, z_i, \lambda)$; that is,

$$E(L, z_i, \lambda) = E_0 - \epsilon(L, z_i, \lambda). \quad (4)$$

It is easy to solve E_0 by using the conventional quantum-mechanical technique.⁸ The eigenvalue $\epsilon(L, z_i, \lambda)$ at the ground state is estimated in a variational manner.

As a tractable trial function to the ground-state eigenfunction of H in Eq. (1), we construct the following:

$$\Psi(\vec{r}) = \begin{cases} Na^{-1/2} e^{\kappa_1(z+L/2)} \Lambda(\rho, z, z_i; \lambda), & z < -L/2 \\ Nk_2^{-1} \sin(k_2 z + \Theta) \Lambda(\rho, z, z_i; \lambda), & -L/2 < z < L/2 \\ -Nb^{-1/2} e^{-\kappa_3(z-L/2)} \Lambda(\rho, z, z_i; \lambda), & z > L/2 \end{cases} \quad (5)$$

where N is the normalization factor and

$$\kappa_1 = \frac{1}{\hbar} [2m^*(A - E_0)]^{1/2}, \quad (6a)$$

$$k_2 = \frac{1}{\hbar} (2m^*E_0)^{1/2}, \quad (6b)$$

$$\kappa_3 = \frac{1}{\hbar} [2m^*(B - E_0)]^{1/2}, \quad (6c)$$

$$\Theta = \frac{k_2 L}{2} + \sin^{-1} \left[\frac{\hbar k_2}{(2m^*A)^{1/2}} \right] \\ = -\frac{k_2 L}{2} - \sin^{-1} \left[\frac{\hbar k_2}{(2m^*B)^{1/2}} \right] + \pi, \quad (6d)$$

$$\Lambda(\rho, z, z_i; \lambda) = \exp\{-[\rho^2 + (z - z_i)^2]^{1/2} / \lambda\}. \quad (6e)$$

It is easily understood that this trial function consists of the eigenfunction of the Hamiltonian (1) without the impurity potential and the hydrogenic $1s$ function containing the variational parameter λ . So this trial function is expected to sufficiently reflect the actual impurity state in the $\text{Ga}_{1-x}\text{Al}_x\text{As-GaAs-Ga}_{1-y}\text{Al}_y\text{As}$ superlattice.

We next calculate the expectation value of the Hamiltonian H , that is,

$$\epsilon(L, z_i, \lambda) = \int_V \Psi^* H \Psi dV. \quad (7)$$

Under given values of L and z_i , we decide the variational parameter λ numerically so as to minimize the eigen-

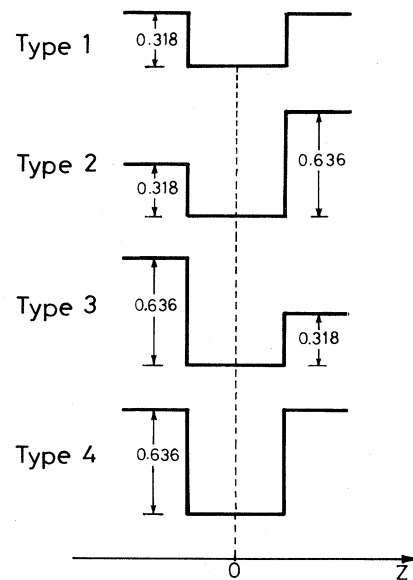


FIG. 2. Schematic representation of the structure of the quantum well with various well heights (in eV) for Table I.

TABLE I. Reduced binding energy in the different well structure with various impurity locations (see Fig. 2).

| $-z_i$ (Å) | Impurity location $\frac{ z_i }{a_0^*}$ | Reduced impurity binding energy (eV) | | | |
|---|--|--------------------------------------|--------------|--------------|--------------|
| | | Type 1 | Type 2 | Type 3 | Type 4 |
| 0.0 | 0 | 2.06(81.6) | 2.08(81.0) | 2.08(81.0) | 2.11(80.2) |
| 23.7 | $\frac{1}{4}$ | 1.79(89.2) | 1.84(87.6) | 1.75(90.8) | 1.80(89.0) |
| 47.4 | $\frac{1}{2}$ | 1.28(116.8) | 1.31(114.8) | 1.23(121.4) | 1.26(119.4) |
| 71.1 | $\frac{3}{4}$ | 0.962(150.0) | 0.980(148.0) | 0.936(154.0) | 0.952(152.5) |
| 94.8 | 1 | 0.782(177.3) | 0.793(176.4) | 0.766(181.5) | 0.776(179.9) |
| 284.3 | 3 | 0.342(334.0) | 0.344(333.0) | 0.340(336.5) | 0.342(335.0) |
| ϵ_0 (The eigenenergy without the impurity) | | 0.03765 | 0.04029 | 0.04029 | 0.04324 |

ergy ϵ . In the present model it is convenient to define the reduced binding energy $E(L, z_i, \lambda)/R_0^*$, where R_0^* is the effective binding energy of the bulk GaAs, given by

$$R_0^* = \frac{m^* e^4}{2\epsilon^2 \hbar^2}. \quad (8)$$

For the same reason, we have similarly scaled the impurity site as z_i/a_0^* where a_0^* is the effective Bohr radius of the bulk GaAs, given by

$$a_0^* = \frac{\epsilon \hbar^2}{m^* e^2}. \quad (9)$$

The values of R_0^* and a_0^* are calculated to be 6.33×10^{-10} eV and 94.8 Å, respectively, for GaAs. The value of a_0^* is employed for that of L for the sake of convenience, in order to make a comparison with the previous study, with the neglect of the tunneling effect of the electron into the

regions I and III.² Another reason for this choice is that the actual superlattices are made to have such a value of L , that is, about 100 Å.^{5,9}

For the barrier heights of the well (A and B), the four kinds of the combinations of the values 0.318 and 0.636 eV were chosen; that is, the components x, y of the content of Al in regions I and III were chosen as the combinations of 0.3 and 0.6 [see Eqs. (3c) and (3d)]. In order that the barriers might be efficient for the conduction electron in region II, the value of the wall height should be more than about 300 meV, which is generally greater than the kinetic energy of the conduction electron.

III. RESULTS AND DISCUSSION

The results in the four kinds of different well structure illustrated in Fig. 2 are listed in Table I with respect to the reduced binding energy with each impurity location. The variational parameters λ_{\min} that make the binding energy minimum are also shown in parentheses in each column.

A. Binding energy and electron density ($x=y=0.3$)

First, let us discuss the results obtained in the case of the finite barrier height in comparison with that in the infinite barrier height previously presented.² In Fig. 3, for instance, the case of $A=B=0.318$ eV ($x=y=0.3$) is plotted with that of $A=B=\infty$. It is clearly seen that the earlier work, which neglects the tunneling effect across the interface between regions II ($|z_i| < L/2$) and I ($z_i < -L/2$), has underestimated the binding energy by the impurity located in the region I. Hence it is obvious that one ought to take the tunneling effect into consideration in order to discuss the binding energy of an injected electron from the impurity outside the quantum well in the superlattice.

On the contrary, the present values of the reduced binding energy considerably decrease in most locations of the impurity inside region II. In the case of the infinite barrier height of the $\text{Ga}_{1-x}\text{Al}_x\text{As}$ layer, an electron, once provided by the hydrogenic impurity, becomes confined in the region II much more often than in the present case.

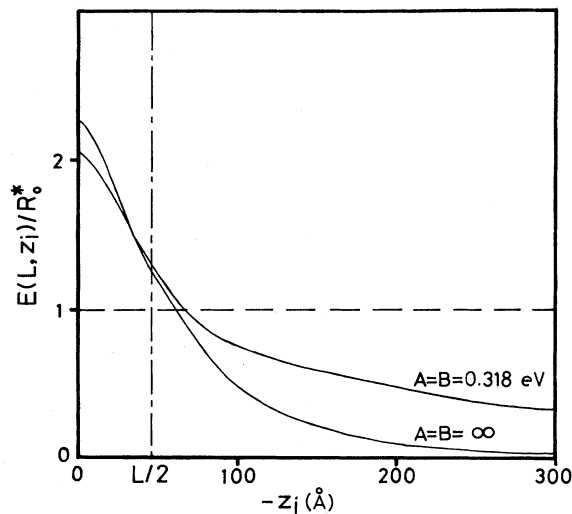


FIG. 3. Dependency of the binding energy on the impurity position: (a) in the case of a finite barrier well ($A=B=0.318$ eV, that is, $x=y=0.3$), and (b) in the case of an infinite barrier well (Ref. 2). There is an interface between regions I and II at $-z_i=L/2$ ($L=a_0^*=94.8$ Å).

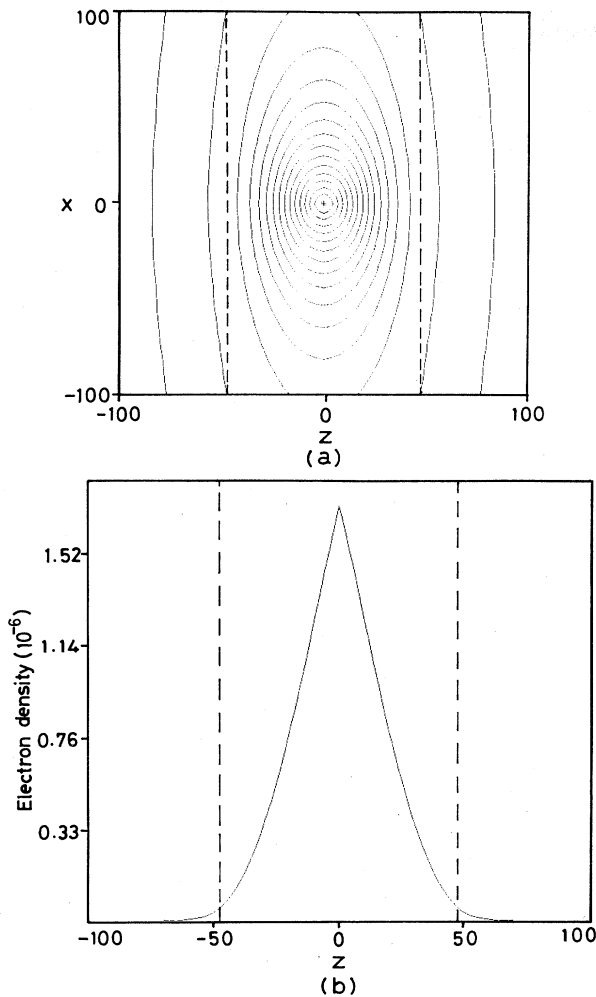


FIG. 4. Electron density distribution with the impurity located at $|z_i| = 0.0 \text{ \AA}$ in the superlattice well. (a) The contour map including the z axis (see the coordinate system in Fig. 1). The $+$ indicates the site of the impurity and the vertical broken lines designate the interfaces between the regions I and II. (b) The longitudinal cross section of the contour map; (a), in regard to the y - z plane (throughout Figs. 4–9). In (a) the density values of the sixteen contours from the outside are 1.0×10^{-10} , 1.0×10^{-8} , 1.0×10^{-7} , 2.0×10^{-7} , 3.0×10^{-7} , 4.0×10^{-7} , 5.0×10^{-7} , 6.0×10^{-7} , 7.0×10^{-7} , 8.0×10^{-7} , 9.0×10^{-7} , 1.0×10^{-6} , 1.1×10^{-6} , 1.2×10^{-6} , 1.3×10^{-6} , 1.4×10^{-6} , in order.

This is the reason why the present finite model gives a considerable decrease in the binding energy when the impurity locates in region II, although this tendency becomes vague as the impurity approaches the interface between the regions II and I.

In Figs. 4(a)–9(a), we show the contour maps of the electron densities in the superlattice depending on various impurity locations. We set the well barrier heights A, B again to be 0.318 eV . The broken lines indicate the interface between the $\text{Ga}_{1-x}\text{Al}_x\text{As}$ layer (region I or III) and the GaAs layer (region II), the $+$ indicating the site of the impurity. The site of the impurity was varied along

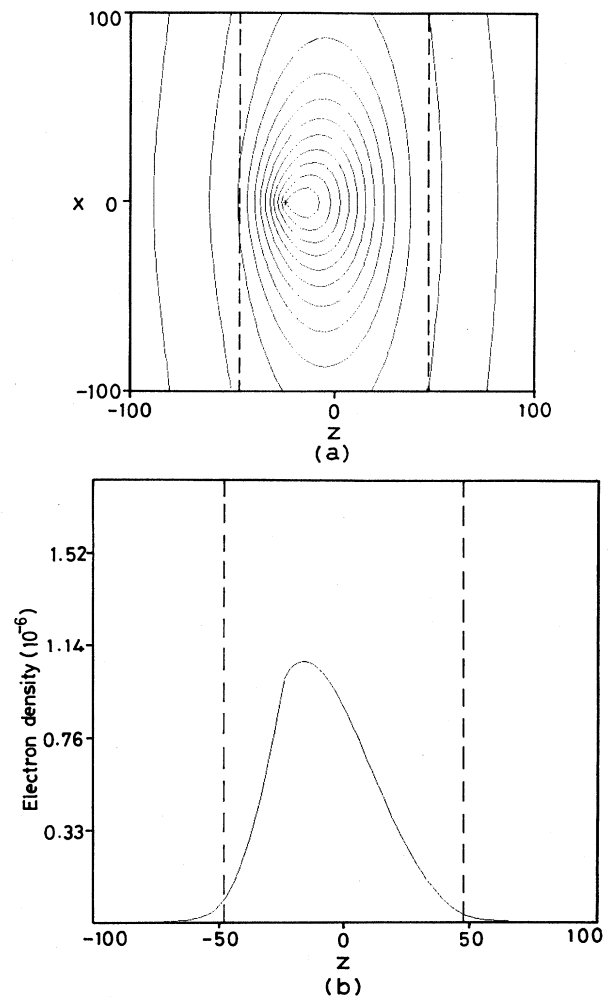


FIG. 5. Impurity located at $|z_i| = L/4$ (i.e., 23.7 \AA) in the superlattice well. In (a) the density values of the twelve contours from the outside are 1.0×10^{-10} , 1.0×10^{-8} , 1.0×10^{-7} , 2.0×10^{-7} , 3.0×10^{-7} , 4.0×10^{-7} , 5.0×10^{-7} , 6.0×10^{-7} , 7.0×10^{-7} , 8.0×10^{-7} , 9.0×10^{-7} , 1.0×10^{-6} , in order.

the z axis from its origin to the minus direction. In the present calculation the x - z plane is taken to be the projection plane (see Fig. 1).

On the other hand, Figs. 4(b)–9(b) directly show the shapes of the same electron densities in order to emphasize the difference of the density of each case. These are equal to the longitudinal cross sections of the upper maps [Figs. 4(a)–9(a)] in regard to the y - z plane.

Figure 4 shows the case with the impurity located at $z_i = 0.0 \text{ \AA}$, the center of the well (i.e., in the GaAs layer). In Fig. 4(a), there are sixteen contours, and the most outside one (namely, the lowest) corresponds to $1.0 \times 10^{-10} (e/\text{\AA}^3)$ throughout this paper, as in the following figures. It is seen that the impurity located at the center of the well naturally attracts the electron.

In Fig. 5, the impurity is located at the $|z_i| = L/4$ (i.e., 23.7 \AA), that is, still inside the well. The most-inside contour in Fig. 5(a) shows the density of 1.0×10^{-6} . One can

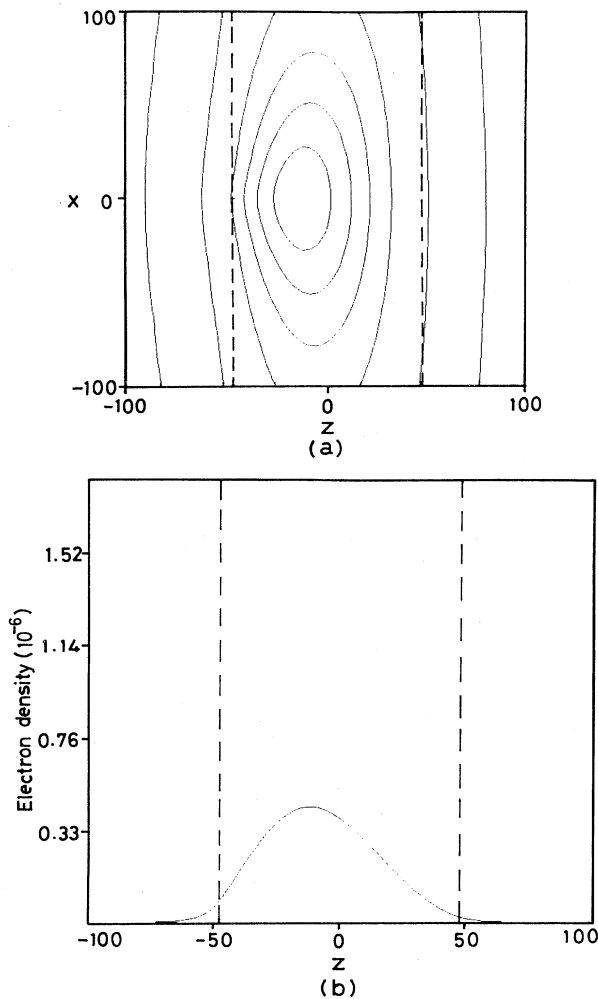


FIG. 6. Impurity located at $|z_i| = L/2$ (i.e., 47.4 Å) in the superlattice well. In (a) the density values of the six contours from the outside are 1.0×10^{-10} , 1.0×10^{-8} , 1.0×10^{-7} , 2.0×10^{-7} , 3.0×10^{-7} , 4.0×10^{-7} , in order.

see that the slight eccentricity of the impurity location induces a considerable reduction of the density peak, and the impurity seems to drag the density influentially. But the left wall of the well compresses the electron density, so the contours are dense between the left wall and the impurity. Accordingly, the density distribution in this situation expresses very well the effect resulting from the cooperation of the attractive Coulomb center and the well structure in the superlattice.

Next, Fig. 6 shows the electron density with the impurity located at $|z_i| = L/2$ (i.e., 47.4 Å), namely just on the interface. In Fig. 6(a), there are six contours and the most inside one shows the density of 4.0×10^{-7} . Compared with Fig. 4, it is seen that the effect of the well structure is rather dominant than the attraction of the impurity existing on the interface. That is to say, the shape in Fig. 6(b) is much smoother than the Figs. 4 and 5, and the electron is fairly well distributed over the wider area. However, it is also noticed that the electron density is

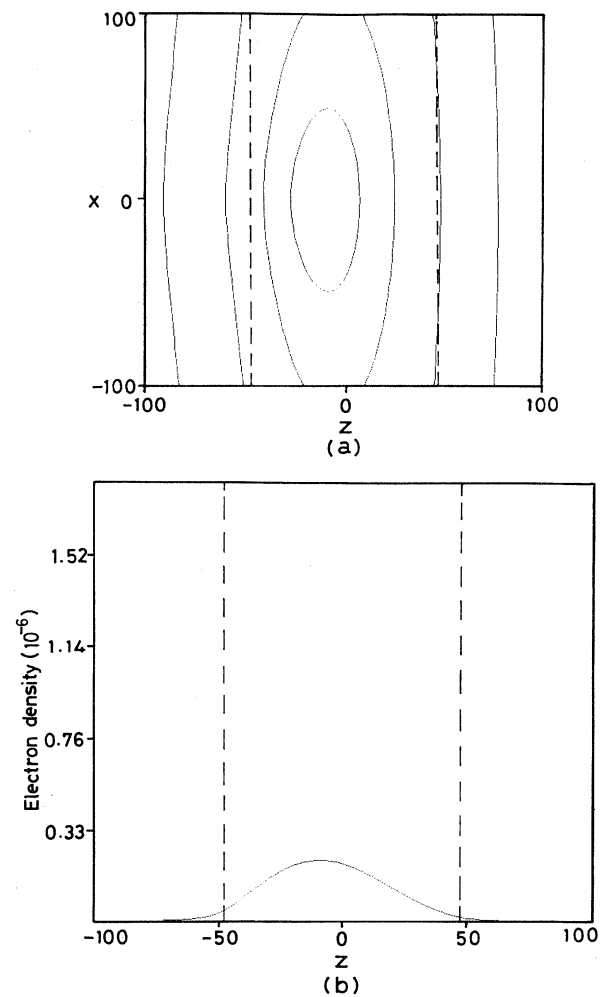


FIG. 7. Impurity located at $|z_i| = 3L/4$ (i.e., 71.1 Å) in the superlattice well. In (a) the density values of the four contours from the outside are 1.0×10^{-10} , 1.0×10^{-8} , 1.0×10^{-7} , 2.0×10^{-7} , in order.

mainly spread over along x and y directions throughout the GaAs layer sandwiched between two $\text{Ga}_{1-x}\text{Al}_x\text{As}$ layers. It is as far as this location that the impurity attraction of the density acts effectively. This will be clarified from the following figures describing the cases of the impurity locations out of the well.

Figure 7 sketches the electron density with the impurity located at the $|z_i| = 3L/4$ (i.e., 71.7 Å). In Fig. 7(a) the most-inside contour corresponds to 2.0×10^{-7} , and one can see the electron spreads wider than Figs. 4–6.

There only exist three contours in Fig. 8(a), in which the impurities located at the $|z_i| = L$ (i.e., 94.8 Å), and the most-inside contour shows 1.0×10^{-7} , being $\frac{1}{14}$ as large as Fig. 4(a). It is seen that the impurity attraction is fairly weak.

In Fig. 9 the impurity is far from the well, that is, located at the point of $|z_i| = 3L$ (i.e., 284.3 Å). (Hence the + mark indicating the impurity site is out of the drawing.) The electron density is distributed very widely along

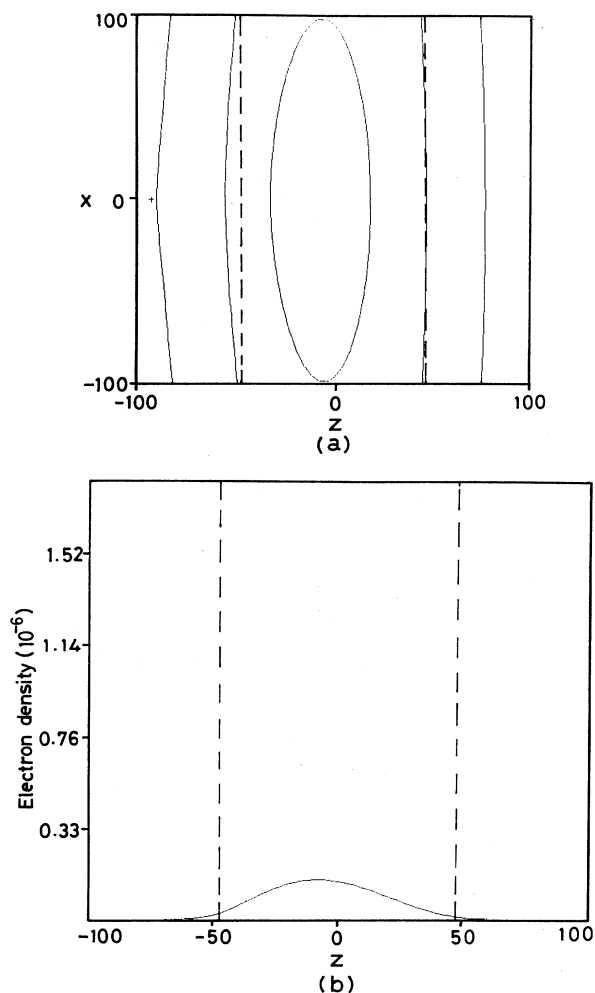


FIG. 8. Impurity located at $|z_i| = L$ (i.e., 94.8 Å) in the superlattice well. In (a), the density values of the three contours from the outside are 1.0×10^{-10} , 1.0×10^{-8} , 1.0×10^{-7} , in order.

the GaAs layer, and the contours in Fig. 9(a) are almost parallel to each other along the interface between the GaAs layer and the $\text{Ga}_{1-x}\text{Al}_x\text{As}$ layers. The peak in Fig. 9(b) is $\frac{1}{140}$ as large as that in Fig. 4(b).

B. Binding energy for other combinations of x and y

Next, let us examine the results for other three different well barrier heights in Table I. Prior to the discussion, we ought to mention the physical meaning of our variational parameter λ in Eq. (5). This parameter is introduced as the denominator of the exponent of the second exponential term (6e). Since the numerator is equal to the distance of the electron from the Coulomb center, we could interpret the optimal variational parameter λ_{\min} as the measure of the extent of the electron density distribution. This interpretation is very similar to that case in the most fundamental treatment of the hydrogen atom, which has the spherical symmetry, where the correspondent becomes exactly the Bohr radius. Accordingly, the variational pa-

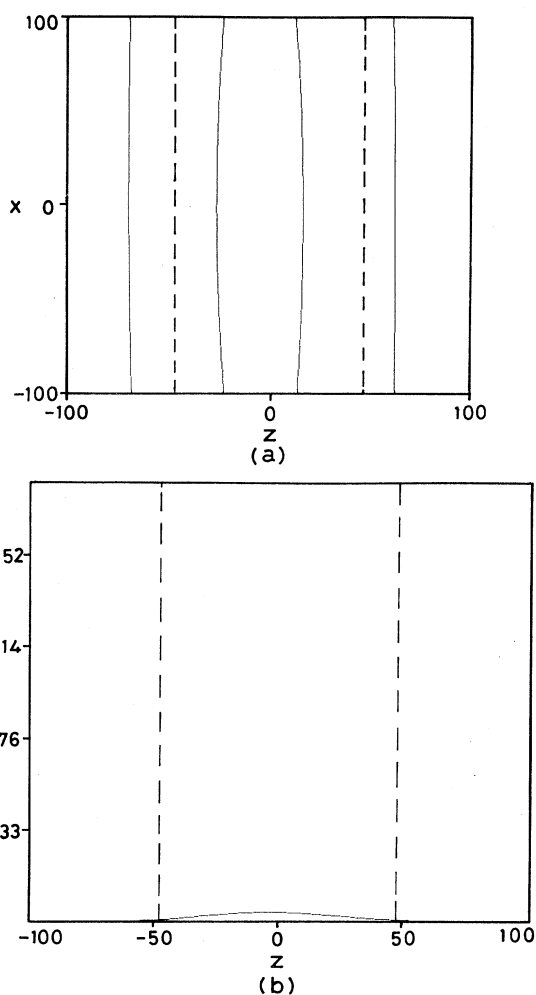


FIG. 9. Impurity located at $|z_i| = 3L$ (i.e., 284.3 Å) in the superlattice well. In (a) the density values of the two contours from the outside are 1.0×10^{-10} , 1.0×10^{-8} , in order.

rameter λ has the dimension of the length. As a matter of course, due to the anisotropy of the model superlattice with an impurity, λ_{\min} does not simply correspond to the effective Bohr radius in the superlattice. However, as shown later, the λ_{\min} is qualitatively a good criterion of the extent of the electron density distribution.

The result in the case of the impurity located at the center in the well in Table I shows that the value of the reduced binding energy is purely affected by each well structure, namely, in cooperation with the left and the right walls of the well interdependently. Thus, in this case, the height of the barrier of the well definitely decides the binding energy.

On the other hand, the cases of $z_i \neq 0$ are not so simple as mentioned above. Figure 10 shows the schematic drawing of the binding energy. The circles indicate the crossing points of the binding energy. It is interesting to note that the four kinds of the binding energy change their orders one after another according to the impurity locations concerned.

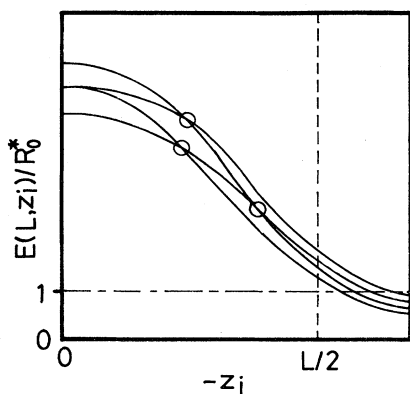


FIG. 10. Schematic feature of the binding energy with different barrier types (see Table I). Circles emphasize the crossing points of the binding energy.

In the cases that the impurity is located outside the well, which we are now most interested in, the well structure of type 3 (see Table I) is the most effective for the modulation doping. For example, in the case of the $|z_i| = 94.8 \text{ \AA}$, the reduced binding energy is less than 1.0, the value in the bulk GaAs layer. The increasing tendency of the value of the optimal variational parameter λ_{\min} is due to the extent of the electron distribution along the GaAs layer and then the electron injected into the region II shows the nature of the quasi-two-dimensional electron gas.

IV. CONCLUDING REMARKS

We have studied the binding energy of the first impurity level in a finite barrier height well, which is supposed to represent the realistic $\text{Ga}_{1-x}\text{Al}_x\text{As-GaAs-Ga}_{1-y}\text{Al}_y\text{As}$ superlattice. It was made clear that in the case of the modulation doping the values of the binding energy are fairly larger than those previously obtained with the use of an infinite-well model.² There still remains, however, a considerable relief from the Coulomb attraction of the impurity center, located out of the well because of the superlattice structure, in comparison with the bulk GaAs layer, which explains well the appearance of the conduction carriers with a higher mobility in actual superlattice.⁵

We have also studied the effect resulting from the anisotropy of the superlattice itself upon the electron distribution. Although it seems that a slight difference between two well barrier heights does not cause much change in regard to the binding energy, some results about the relation between the impurity location and the heights of the two barriers existing in the interfaces were obtained. It can be suggested that these results would propose a kind of guide to prepare devices using superlattices.

ACKNOWLEDGMENTS

One of the authors (K.T.) wishes to thank Dr. Raphael Tsu for his stimulating discussion. One of us (M.N.) would like to thank Dr. Tsutomu Minato for his suggestion in regard to the computer programs. Numerical calculations were carried out at the Data Processing Center of Kyoto University and the Computer Center of Institute for Molecular Science, Okazaki, Japan.

¹L. Esaki and R. Tsu, *IBM J. Res. Develop.* **14**, 61 (1970).

²G. Bastard, *Phys. Rev. B* **24**, 4714 (1981).

³C. Mailhot, Yia-Chung Chang, and T. C. McGill, *Phys. Rev. B* **26**, 4449 (1982).

⁴R. L. Greene and K. K. Bajaj, *Solid State Commun.* **45**, 825 (1983).

⁵R. Dingle, H. Störmer, A. C. Gossard, and W. Wiegmann,

Appl. Phys. Lett. **33**, 665 (1978).

⁶D. J. BenDaniel and C. B. Duke, *Phys. Rev.* **152**, 683 (1966).

⁷W. A. Harrison, *Phys. Rev.* **123**, 85 (1961).

⁸A. Messiah, *Quantum Mechanics* (North-Holland, Amsterdam, 1961).

⁹J. P. van der Ziel, R. Dingle, R. C. Miller, W. Wiegmann, and W. A. Nordland Jr., *Appl. Phys. Lett.* **26**, 463 (1975).